ON BERNOULLI'S METHOD*

TAMÁS DÓZSA†, FERENC SCHIPP‡, AND ALEXANDROS SOUMELIDIS§

Abstract. We generalize Bernoulli's classical method for finding poles of rational functions using the rational orthogonal Malmquist-Takenaka system. We show that our approach overcomes the limitations of previous methods, especially their dependence on the existence of a so-called dominant pole, while significantly simplifying the required calculations. A description of the identifiable poles is provided, as well as an iterative algorithm that can be applied to find every pole of a rational function. We discuss automatic parameter choice for the proposed algorithm and demonstrate its effectiveness through numerical examples.

Key words. Bernoulli's method, rational functions, Malmquist-Takenaka system, pole identification

MSC codes. 65T65, 30E10, 41A20

1. Introduction.

Numerical methods focusing on rational approximation and interpolation have provided a rich area of research in the last decades [12, 22, 27, 37, 38, 39]. Many fields, such as control and system theory [39] and partial differential equations [12, 22, 27, 37, 38] have benefited from such approaches. In this work, we discuss the problem of finding the poles of rational functions by generalizing a method known as Bernoulli's method. As we later point out the proposed methods have great application potential especially in the field of system identification. Daniel Bernoulli considered the problem of finding the dominant (largest in absolute value) zero of a polynomial P. Identifying the zeros of the n-th degree polynomial P is equivalent to finding the poles of the rational function $R(z) := \frac{1}{z^n P(1/z)}$. Supposing that R has a unique dominant pole (the smallest in absolute value) outside the closed disk $\overline{\mathbb{D}}$, the ratios c_{n+1}/c_n constructed from the coefficients of the expansion

$$R(z) = \sum_{n=0}^{\infty} c_n z^n \qquad (|z| \leq 1) \tag{1.1}$$

converge to this dominant pole [15]. In (1.1), the coefficients c_n are the Fourier-coefficients of R with respect to the trigonometric system [11].

We now proceed to give a brief historical background about this method based on the monographs [14] and [17]. Bernoulli calculated c_n in (1.1) using a recursion applied to the coefficients of P. We note that using the terminology of system theory, the Fourier-coefficients c_n can also be interpreted as the impulse response of the SISO

---

*Submitted to the editors on 12.10.2022.

Funding: Project no. C1748701 and K146721 have been implemented with the support provided by the Ministry of Culture and Innovation of Hungary from the National Research, Development and Innovation Fund, financed under the NVKDP-2021 and the K_23 "OTKA" funding schemes, respectively. The research was supported by the European Union within the framework of the National Laboratory for Autonomous Systems. (RRF-2.3.1-21-2022-00002).

†HUN-REN Institute for Computer Science and Control, Systems and Control Laboratory, Budapest, Hungary, Eötvös Lóránd University, Faculty of Informatics, Department of Numerical Analysis, Budapest, Hungary (dozsatamas@sztaki.hu)

‡Eötvös Lóránd University, Faculty of Informatics, Department of Numerical Analysis, Budapest, Hungary (schipp@inf.elte.hu)

§HUN-REN Institute for Computer Science and Control, Systems and Control Laboratory, Budapest, Hungary (soumelidis@sztaki.hu)

(single input single output) [2] system whose transfer function is R. The original idea of Bernoulli was expanded by König, who generalized the pole finding method to meromorphic functions [17, 18]. Since then, many subsequent generalizations have been introduced. We note the work of Aitken, who showed that the determinants of Hankel-matrices created from the coefficients c_n can be used to approximate every pole, provided that the absolute values of the poles are pairwise different [1, 17]. Using the so-called qd (quotient-difference) algorithm, Rutishauser [29, 30] and Henrici [14] further imrpoved Aitken's results. Detailed results on the relationship between Hankel determinants, the product of the poles and the qd algorithm can be found in chapter 7 and chapter 3 of [14] and [17], respectively.

As illustrated in Figure 1, Bernoulli's method diverges if the rational function has more than one dominant pole. We note that the above mentioned generalizations are also prone to this limitation of the method. In addition, this excludes the possibility of using Bernoulli's method for identifying the poles of SISO transfer functions, since realizable systems often have complex conjugate pairs as dominant poles.

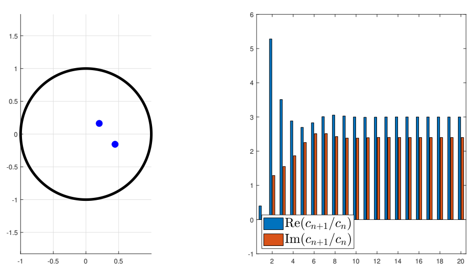

(a) LEFT: Inverse poles (reflections of the poles across the torus) of the rational function (dominant pole uniquely exists). RIGHT: the sequence c_{n+1}/c_n.

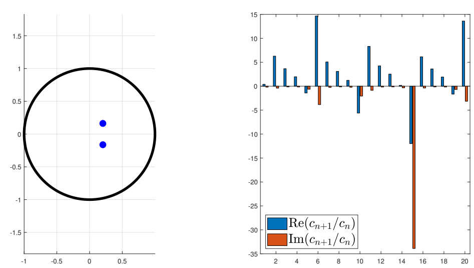

(b) LEFT: Inverse poles of the rational function In this example there is no unique dominant pole. RIGHT: Real and imaginary parts of c_{n+1}/c_n.

Fig. 1: Bernoulli's pole finding method. The sequence c_{n+1}/c_n diverges if the function has multiple dominant poles.

In [32], a generalization of Bernoulli's method was proposed, where the discrete Laguerre-Fourier coefficients of R were considered. Using this approach we can overcome the above mentioned limitation of Bernoulli's algorithm and reconstruct a larger subset of the poles of R. In fact, the algorithm proposed in [32] can be used to reconstruct every dominant pole of R. Later, using the ideas in [32] the von Mieses algorithm, which is capable of finding the dominant eigenvalues of matrices was generalized in [33]. In addition, using the so-called fartherst-point Voronoi mappings [4] induced by the pseudo-hyperbolic metric, we were able to characterize the poles of the function R which can be reconstructed by this method.

The main contribution of this work is a further generalization of the ideas proposed in [32]. Namely, we propose to use the coefficients of periodic Malmquist-Takenaka series [16, 24, 35, 39] to find the inverse poles of R. The proposed methods will include the ideas discussed in [32] as a special case. One important advantage of our generalization is that using the coefficients from a periodic Malmquist-Takenaka expansion, we can construct an iterative algorithm to find every pole of R.

The paper is organized as follows. In section 2 we discuss periodic Malmquist-

Takenaka systems, generalize the concept of dominant poles and introduce a generalization of Bernoulli's algorithm. In section 3 we describe the poles which can be found using the proposed method. In section 4 we consider the problem of discretization. In section 5 we propose an iterative algorithm to identify every pole of a rational function based on periodic Malmquist-Takenaka coefficients. We discuss some numerical considerations of the proposed methods in section 6, then conclude our work with an overview and future plans in section 7.

2. A generalization of Bernoulli's method. In Bernoulli's pole finding method, the coefficients c_n refer to the Fourier coefficients of the rational function R with respect to the trigonometric system $(\epsilon_n,\ n \in \mathbb{Z})$ [11]:

$$c_n = \langle R, \epsilon_n \rangle := \frac{1}{2\pi} \int_0^{2\pi} R(e^{it}) e^{-int} dt \quad (n \in \mathbb{N}).$$

Provided that the function values of R are available on the torus, c_n can be calculated. We note that Bernoulli's method can also be applied using discrete Fourier coefficients instead of c_n. For the elementary rational functions

$$r_\alpha(z) := \sum_{n=0}^{\infty} \overline{\alpha}^n z^n = \frac{1}{1 - \overline{\alpha} z}. \tag{2.1}$$

Bernoulli's algorithm can easily be verified. The number $\alpha^* := 1/\overline{\alpha}$ is the pole of the function r_α. Since α is the reflection of α^* accross the torus $\mathbb{T} := \{z \in \mathbb{C} : |z| = 1\}$, we will refer to α as the inverse pole of r_α henceforth.

Let $\mathcal{A}$ denote the set of analytic functions on the closed disk. The classical Bernoulli method is summarized by the next theorem.

THEOREM 2.1 (Bernoulli's algorithm). *Suppose the multiplicity of each inverse pole of the rational function $R \in \mathcal{A}$ is 1. If $\alpha_0 \in \mathbb{D}$ is the dominant inverse pole of R, or in other words for any $\alpha \neq \alpha_0$ inverse pole, $|\alpha_0| > |\alpha|$ holds, then*

$$\frac{\langle \epsilon_n, R \rangle}{\langle \epsilon_{n-1}, R \rangle} = \alpha_0 + O(q^n), \tag{2.2}$$

where $q = \max_{\alpha_0 \neq \alpha} |\alpha|/|\alpha_0|$.

We note that the convergence also holds when R has higher multiplicity inverse poles, however in this case the rate of convergence is $O(1/n)$.

The main contribution of this paper is the generalization of (2.2) to Malmquist-Takenaka systems generated by periodic sequences (or in short PMT systems), which contain the Laguerre and trigonometric systems as special cases. In this section we introduce a generalized version of (2.2), which allows us to identify a single inverse pole of a rational function. We also generalize the concept of dominant inverse poles and specify the inverse poles which can be found by the proposed method. Later in section 5 we introduce an algorithm based on the findings in this section, which will allow us to iteratively find every inverse pole of the rational function in question.
Malmquist-Takenaka (or MT) systems [24, 35] can be described with the help of Blaschke factor [3]:

$$B_a(z) := \frac{z - a}{1 - \overline{a} z} \qquad (a \in \mathbb{D}, |z| \leq 1). \tag{2.3}$$

It is well-known [25, 31] that every Blaschke factor in

$$\mathfrak{B} := \{\varepsilon B_a : (a, \varepsilon) \in \mathbb{D} \times \mathbb{T}\} \tag{2.4}$$

is a bijection on $\mathbb{D}$ and $\mathbb{T}$, furthermore $\mathfrak{B}$ forms a transformation group on $\mathbb{D}$ with respect to function composition. This group describes the congruence transformations of the Bolyai-Lobachevsky geometry in the Poincaré disc model [6, 34].

The pseudo-hyperbolic distance

$$\rho(a, b) := |B_a(b)| \qquad (a, b \in \mathbb{D}) \tag{2.5}$$

is a metric on $\mathbb{D}$ which shows invariance towards Blaschke-transformations [25, 31]:

$$\rho(T(a), T(b)) = \rho(a, b) \qquad (a, b \in \mathbb{D}, T \in \mathfrak{B}).$$

Every sequence $\mathfrak{a} = (a_n, n \in \mathbb{N}) \in \mathfrak{U} := \mathbb{D} \times \mathbb{D} \times \ldots$ defines the MT-system [24, 36] $\Phi^{\mathfrak{a}} := \{\Phi_n^{\mathfrak{a}} : n \in \mathbb{N}\}$, where

$$\phi_n^{\mathfrak{a}} := \sqrt{1 - |a_n|^2} \;\; r_{a_n} \prod_{j=0}^{n-1} B_{a_j} \qquad (n \in \mathbb{N}, \mathfrak{a} \in \mathfrak{U}). \tag{2.6}$$

It is well-known [16, 31] that MT-functions form a complete function system in the Hardy space $H^2(\mathbb{D})$ if and only if

$$\sum_{n=0}^{\infty} (1 - |a_n|) = \infty.$$

Furthermore, for any $\mathfrak{a} \in \mathfrak{U}$, the function system $\Phi^{\mathfrak{a}}$ is orthogonal with respect to the scalar product in $H^2(\mathbb{D})$ defined as

$$\langle f, g \rangle := \frac{1}{2\pi} \int_0^{2\pi} f(e^{it}) \overline{g(e^{it})} dt \quad (f, g \in H^2(\mathbb{D})). \tag{2.7}$$

We say that the MT system $\Phi^{\mathfrak{a}}$ is p-periodic if there exists a number $p \in \mathbb{N}^* := \{n \in \mathbb{N} : n \geq 1\}$, such that $a_{n+p} = a_n$ $(n \in \mathbb{N})$. Such p-periodic sequences from $\mathfrak{U}$ can be identified with the elements of the space $\mathfrak{U}_p := \mathbb{D}^p$. Periodic MT-systems can be described with p-order Blaschke-products:

$$B_{\mathfrak{a}}(z) = \prod_{j=0}^{p-1} B_{a_j}(z) \qquad (\mathfrak{a} \in \mathfrak{U}_p, \; z \in \overline{\mathbb{D}}). \tag{2.8}$$

Using (2.6) and (2.8) the p-periodic MT functions can be written as

$$\phi_{kp+n}^{\mathfrak{a}} = \phi_n^{\mathfrak{a}} B_{\mathfrak{a}}^k \qquad (0 \leq n < p, k \in \mathbb{N}). \tag{2.9}$$

Using Cauchy's formula, we get that for any $\phi \in \mathcal{A}$ analytic function and elementary rational function (2.1)

$$\frac{1}{2\pi i}\int_{\mathbb{T}} \frac{\phi(z)}{z-\alpha}dz = \langle \phi, r_\alpha\rangle = \phi(\alpha) \quad (\alpha \in \mathbb{D}). \tag{2.10}$$

By (2.10) we can acquire simple formulas for the ratios of the PMT-Fourier coefficients corresponding to the elementary rational function r_α. The special case of choosing a single parameter $\mathfrak{a} = (a)$ $(a \in \mathbb{D})$ yields the so-called discrete Laguerre system [5, 16]. By (2.9) and (2.10) it is easy to see that in this case we have $\langle \phi_k^a, r_\alpha\rangle = \phi_0^a(\alpha) B_a^k(\alpha)$, thus

$$\frac{\langle \phi_k^a, r_\alpha\rangle}{\langle \phi_{k-1}^a, r_\alpha\rangle} = \frac{\phi_k^a(\alpha)}{\phi_{k-1}^a(\alpha)} = B_a(\alpha) \quad (k \in \mathbb{N}^*). \tag{2.11}$$

From (2.11), the inverse pole α can be easily acquired by the inverse B_{-a} of B_a.

We now proceed to propose a pole reconstruction method similar to (2.11) in the general case, when we consider $\mathfrak{a} \in \mathfrak{U}_p$ p-periodic sequences. For example by taking the indices

$$\nu_k := n + pk \quad (k \in \mathbb{N}^*, 0 < n < p, p > 1) \tag{2.12}$$

we get the ratios

$$\frac{\langle \phi_{\nu_k}^{\mathfrak{a}}, r_\alpha\rangle}{\langle \phi_{\nu_k-1}^{\mathfrak{a}}, r_\alpha\rangle} = \frac{\phi_n^{\mathfrak{a}}(\alpha)}{\phi_{n-1}^{\mathfrak{a}}(\alpha)} \quad (k \in \mathbb{N}^*, n > 0, p > 1). \tag{2.13}$$

In (2.13), if we choose $p = 1$ as a special case we get formula (2.11).

Before we can formulate our main claim, we need to generalize the concept of dominant poles. Let $A \subset \mathbb{D}$ be a finite set. We say that $\alpha_0 \in A$ is a $B_{\mathfrak{a}}$-dominant point in A, if

$$|B_{\mathfrak{a}}(\alpha_0)| > |B_{\mathfrak{a}}(\alpha)| \quad (\alpha \in A, \alpha \neq \alpha_0). \tag{2.14}$$

Using (2.13) and (2.14) we can generalize Bernoulli's method with the following theorem.

THEOREM 2.2. *Suppose that the inverse poles $\alpha \in A$ of the rational function R are simple and let α_0 be the $B_{\mathfrak{a}}$-dominant inverse pole of R. Then, the limit*

$$\lim_{k\to\infty} \frac{\langle \phi_{\nu_k}^{\mathfrak{a}}, R\rangle}{\langle \phi_{\nu_k-1}^{\mathfrak{a}}, R\rangle} = \frac{\phi_n^{\mathfrak{a}}(\alpha_0)}{\phi_{n-1}^{\mathfrak{a}}(\alpha_0)} \quad (\mathfrak{a} \in \mathfrak{U}_p, p \geq 1) \tag{2.15}$$

exists and the rate of convergence in (2.15) is $O(q^k)$, where

$$q := \max_{\alpha\in A,\ \alpha\neq\alpha_0} |B_{\mathfrak{a}}(\alpha)|/|B_{\mathfrak{a}}(\alpha_0)|.$$

Proof. Let $R(z) := \sum_{\alpha\in A} \lambda_\alpha r_\alpha(z)$ $\quad (z \in \mathbb{D}\cup\mathbb{T}, \lambda_\alpha \in \mathbb{C})$ be an analytic rational function on the closed disk. Then, by (2.14) $B_{\mathfrak{a}}(\alpha_0) \neq 0$. Furthermore, by (2.9) and (2.10)

$$\begin{aligned}
\langle \phi^{\mathfrak{a}}_{\nu_k}, R\rangle &= \overline{\lambda}_{\alpha_0}\phi^{\mathfrak{a}}_{\nu_k}(\alpha_0) + \sum_{\alpha\in A\setminus\{\alpha_0\}} \overline{\lambda}_{\alpha}\phi^{\mathfrak{a}}_{\nu_k}(\alpha) = \\
&= B^k_{\mathfrak{a}}(\alpha_0)\left(\overline{\lambda}_{\alpha_0}\phi^{\mathfrak{a}}_{n}(\alpha_0) + \sum_{\alpha\in A\setminus\{\alpha_0\}} \overline{\lambda}_{\alpha}\phi^{\mathfrak{a}}_{n}(\alpha)\frac{B^k_{\mathfrak{a}}(\alpha)}{B^k_{\mathfrak{a}}(\alpha_0)}\right) = \\
&= B^k_{\mathfrak{a}}(\alpha_0)\left(\overline{\lambda}_{\alpha_0}\phi^{\mathfrak{a}}_{n}(\alpha_0) + O(q^k)\right),
\end{aligned}$$

from which (2.15) follows directly. We note that, if $A\setminus\{\alpha_0\} = \emptyset$, then $q = 0$ and the sequence (2.15) is constant. □

We note that a similar statement can be formulated for inverse poles with higher multiplicities, however in this case the rate of convergence cannot be guaranteed unless the multiplicity of α_0 remains 1. Due to the special choice of the indices ν_k the above ratios can be written as

$$S(z) = S^{\mathfrak{a}}_n(z) = \frac{\phi^{\mathfrak{a}}_n(z)}{\phi^{\mathfrak{a}}_{n-1}(z)} = \kappa_n\frac{z-a_{n-1}}{1-\overline{a}_n z}, \tag{2.16}$$

where

$$\kappa := \kappa_n := \sqrt{(1-|a_n|^2)/(1-|a_{n-1}|^2)} \quad (z\in\mathbb{D}, 0\le n\le p-1).$$

We can easily invert $w = S(z)$ with the formula

$$z = Q(w) = Q^{\mathfrak{a}}(w) = \frac{w/\kappa + a_{n-1}}{1+\overline{a}_n w/\kappa}. \tag{2.17}$$

Using the limit $s(\mathfrak{a}) := \lim_{k\to\infty} s_k(\mathfrak{a})$, where

$$s_k(\mathfrak{a}) = s^R_k(\mathfrak{a}) := \frac{\langle \phi^{\mathfrak{a}}_{\nu_k}, R\rangle}{\langle \phi^{\mathfrak{a}}_{\nu_{k-1}}, R\rangle}\ (k\in\mathbb{N}^*), \tag{2.18}$$

we can rewrite (2.15) as

$$\alpha_0 = Q^{\mathfrak{a}}(s(\mathfrak{a})). \tag{2.19}$$

In practice, applying formula (2.19) comes at the cost of numerical errors. The cause of these errors is that in practice we can only consider the value of s_{m^*} (for some finite m^* index) instead of the limit s. This error can be expressed by

$$|Q^{\mathfrak{a}}(s(\mathfrak{a})) - Q^{\mathfrak{a}}(s_{m^*}(\mathfrak{a}))| \le M(\mathfrak{a})\cdot|s(\mathfrak{a}) - s_{m^*}(\mathfrak{a})|, \tag{2.20}$$

where $M(\mathfrak{a}) := \max_{w\in S(\overline{\mathbb{D}})}|Q'(w)|$. The value of $Q'(w)$ can be expressed at a point $w = S(z)$ as

$$Q'(w) = \frac{1}{S'(z)} = \frac{(1-\overline{a}_n z)^2}{\kappa(1-a_{n-1}\overline{a}_n)},$$

from which we get

$$M(\mathfrak{a}) = \frac{(1+|a_n|)^2}{\kappa|1-a_{n-1}\overline{a}_n|}. \tag{2.21}$$

Practical ways to choose the parameter $\mathfrak{a}$ and estimate $|s(\mathfrak{a}) - s_{m^*}(\mathfrak{a})|$ are discussed in section 6.

We note that in the special case $p = 1$, we choose $a_{n-1} = a_n = a$ in the above formulas. We would like to highlight that choosing $\mathfrak{a} = (0)$ yields $\phi_n^0(z) = z^n$, the trigonometric system and in this case α_0 is the dominant inverse pole in the usual sense. In this case equation (2.14) also has an obvious geometrical interpretation.

Considering the 1-periodic parameter sequence $\mathfrak{a} = (a)$ $(a \in \mathbb{D})$ produces the discrete Laguerre-system and condition (2.14) becomes

$$\rho(a,\alpha_0) = |B_a(\alpha_0)| > |B_a(\alpha)| = \rho(a,\alpha) \quad (\alpha \in A), \tag{2.22}$$

where $\rho(\cdot,\cdot)$ is the pseudo-hyperbolic metric as given in (2.5). We discuss the geometric interpretation of (2.22) in [32]. We note that in this special case $n = 1,\ a_0 = a_1 = a$, therefore

$$M(a) = \frac{(1+|a|)^2}{1-|a|^2} = \frac{1+|a|}{1-|a|}.$$

3. Geometric properties of dominant poles. In this section we summarize the geometric interpretations of the generalized dominant poles (2.14). From the point of view of our proposed pole identification scheme built around theorem 2.2, the results in this section help us visualize how to choose the parameters of the Malmquist-Takenaka expansions to identify specific poles of the rational function R. Formally, using the concept of Voronoi-mappings [4], we describe some regions of $\mathbb{D}$. Choosing the parameters of the aforementioned MT-systems from these regions and applying theorem 2.2 will allow for finding specific poles of R. The results discussed here also show, that some poles may be "hidden" in the sense, that independent of our choice of the parameter vector $\mathfrak{a}$, they will never be dominant (will not satisfy (2.14)), therefore cannot be recovered directly using theorem 2.2. In order to find such hidden poles with the proposed method, "cancelling the effect" of other poles is necessary. We discuss such techniques in section 5.

We begin by considering the $p = 1$ case, that is, when the periodic Malmquist-Takenaka system in theorem 2.2 depends on a single $a \in \mathbb{D}$ parameter. We are going to illustrate that in this case, the dominant poles of R can be described using the so-called pseudo hyperbolic metric and Voronoi mappings. Moreover, we are going to investigate an interesting relationship between these dominant, or "visible" poles (the ones that we can recover using theorem 2.2), and the extreme points of the convex hull of the inverse poles. This observation will allow us to point out some interesting relationships between Voronoi-mappings generated by different types of metrics and corresponding variants of convex hulls. The notion of dominant poles as introduced in [32] can be geometrically described using farthest-point Voronoi-mappings [4]. Let F_A denote the union of the hyperbolic bisectors $\ell_{a,b} := \{z \in \mathbb{D} : \rho(a,z) = \rho(b,z)\}$ and let $D_A := \mathbb{D} \setminus F_A$ $(a,b \in A, a \neq b)$. Then, for each $a \in D_A$ there uniquely exists a point $\alpha \in A$ which is farthest from a in metric ρ. Let $V = V_A := D_A \to A$ denote the function which maps every $a \in D_A$ to the point in A farthest away from it. Then, V_A

is the farthest-point Voronoi mapping of the set A generated by the pseudo hyperbolic distance. The $V_A^{-1}(\alpha)$ $(\alpha \in A)$ Voronoi-cells provide a disjoint partitioning of the set $\mathbb{D} \setminus A$. Condition (2.22) is equivalent to $V_A(a) = \alpha_0$, that is the set of inverse poles which are B_a $(a \in \mathbb{D})$ dominant is exactly the range of the Voronoi mapping V_A. Any inverse poles α for which $V_A^{-1}(\alpha) = \emptyset$ cannot be retrieved.

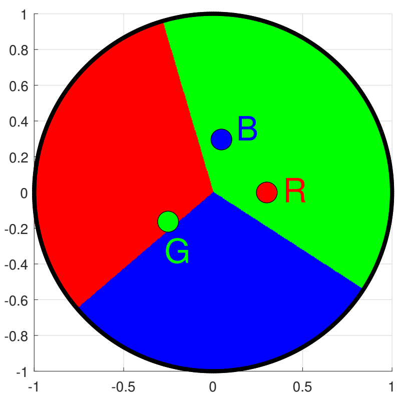

(a) Farthest-point Voronoi diagram using pseudo hyperbolic distance. In this case there were more than one dominant inverse poles in the classical sense, however using the proposed approach (2.15), we can reconstruct any of them.

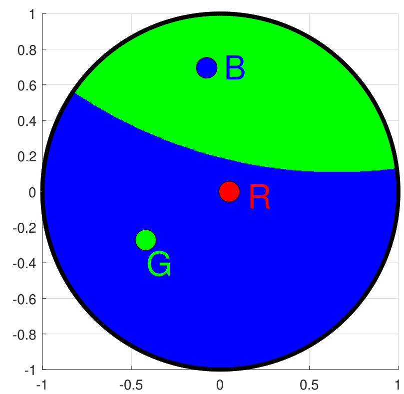

(b) Farthest-point Voronoi diagram using pseudo hyperbolic distance. Not every $a \in A$ is guaranteed to have a nonempty Voronoi cell. In this case the point labeled "R" has no corresponding region.

Fig. 2: Some example Voronoi cells generated by the pseudo hyperbolic distance. Members of the set A are denoted by points of different colors and are labeled with the letters "R", "G" and "B" for red, green and blue. The corresponding Voronoi cells are shown in the same color. If A contains the inverse poles of a rational function R, then choosing the parameter of the 1-periodic MT system (discrete Laguerre system) from the set $V_A^{-1}(\alpha)$ $(\alpha \in A)$ allows for the reconstruction of the inverse pole α with (2.15).

In figure 2, we illustrate some farthest-point cells $V_A^{-1}(\alpha)$. For the examples in figure 2, not considering points strictly on the border between two neighbouring Voronoi cells, the limit (2.15) exists for any $a \in \mathbb{D}$ parameter. The rate of convergence depends on the choice of the parameter a choosen from the Voronoi-cells. The choice of this parameter will be further discussed in section 6. Suppose that A contains the inverse poles of a rational function. Then, the examples in figure 2 also illustrate that if there is no dominant inverse pole (the points in A fall on a circle), each inverse pole can still be found using the proposed algorithm.

We note that in the Euclidean plane (when we define the distance generating the Voronoi mappings as $\rho(a, b) = \|a - b\|_2$ $(a, b \in \mathbb{R}^2)$ instead of (2.5)), we can describe V_A using convex geometry. Namely, the range of V_A can be described by the set of extreme points of the convex hull of A (see figure 4). The analogous statement does not hold for the hyperbolic case. In figure 4, we illustrate that the set of vertices of the hyperbolic convex hull of A is larger than the range of V_A. In this case, one can describe the range of V_A on the hyperbolic plane using the notion of paracyclic convexity. We plan to investigate this phenomena in detail in a future work.

Next, we would like to extend the idea of describing the dominant (or "visible") inverse poles of the rational function R for identification by periodic MT-systems, where $p \geq 2$. In this case, the MT-Fourier coefficients used to identify the dominant inverse poles depend on a p dimensional parameter vector denoted by $\mathfrak{a}_p$. We are interested in describing the Voronoi cells generated by the inverse poles of R, where instead of the hyperbolic metric discussed above, the notion of distance is given by the Blaschke product corresponding to $\mathfrak{a}_p$. The case, when the first $p-1$ components in $\mathfrak{a}_p$ are chosen as the inverse poles $\alpha_0, \ldots, \alpha_{p-2} \in A$ will be of special interest to us (see figure 3 and section 5), however we discuss our findings for a general choice of $\mathfrak{a}$. In order to give a geometric description of the general case, let us consider the sequence $\mathfrak{a} := (a_0, a_1, \ldots) \in \mathfrak{A}$ and fixing the first $p-1$ components define

$$\mathfrak{a}_p := (a_0, a_1, \ldots, a_{p-2}, a) \quad (a \in \mathbb{D}). \tag{3.1}$$

We are going to use the vector $\mathfrak{a}_p$ to construct a periodic MT system. Then, as stated in (2.14), we call $\alpha_0 \in A$ the $B_{\mathfrak{a}_p}$-dominant element in A if for the mapping

$$\rho_p(a, \alpha) := |B_{\mathfrak{a}_p}(\alpha)| \ (\alpha \in \mathbb{D}), \tag{3.2}$$

the statement analogous to (2.14) holds:

$$\rho_p(a, \alpha_0) > \rho_p(a, \alpha) \ (\alpha \in A, \alpha \neq \alpha_0). \tag{3.3}$$

Using the mappings ρ_p we can introduce the Voronoi mappings $V_{A,p}$ generated by them. For any interior point of the Voronoi cells, the limit (2.15) exists. We note that if $\alpha \in A$ and α is also a component in $\mathfrak{a}_p$, then $V_{A,p}^{-1}(\alpha) = \emptyset$, or in other words α cannot be found using the proposed method. As discussed in detail in section 5, this property can be exploited to construct an iterative algorithm which finds every pole of the rational function. An example mapping $V_{A,p}$ is provided for $p = 2$ in figure 3.

4. Discrete Malmquist-Takenaka systems. In numerical calculations instead of the Fourier coefficients $\widehat{f}(n)$ [11] of a function $f : \mathbb{T} \to \mathbb{C}$ we often consider the N-periodic discrete Fourier-coefficients

$$\widehat{f}_N(n) := \frac{1}{N} \sum_{z \in \mathbb{T}_N} f(z) z^{-n} \qquad (n, N \in \mathbb{N} \setminus \{0\}), \tag{4.1}$$

where

$$\mathbb{T}_N := \{e^{2i\pi k/N} : 0 \leq k < N\}.$$

The (finite) trigonometric system is orthogonal with respect to the discrete inner product [11]

$$[f, g]_N := \frac{1}{N} \sum_{z \in \mathbb{T}_N} f(z) \overline{g}(z) \qquad (N = 2, 3, \ldots).$$

Let $\widehat{r}_\alpha(n)$ denote the n-th Fourier coefficient of the elementary rational function r_α. From the formula

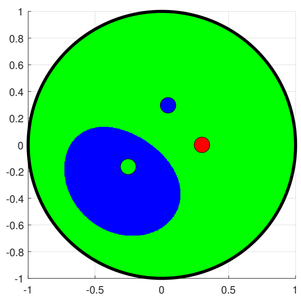

Fig. 3: An example of $V_{A,p}$ for $p = 2$. For $p > 1$, the borders between the Voronoi cells can no longer be described with hyperbolic lines. In this case a_0 is chosen as the inverse pole denoted by the red point (hence its corresponding Voronoi cell is empty). If we choose the parameter a_1 from either of the two Voronoi cells and apply theorem 2.2, then we can find the inverse pole corresponding to the color of the chosen cell.

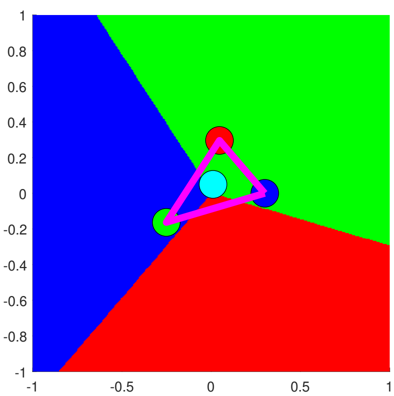

(a) Farthest-point Voronoi mapping on the Euiclidean plane (generated by Euclidiean distance). The set of vertices of the convex hull of A is the range of V_A.

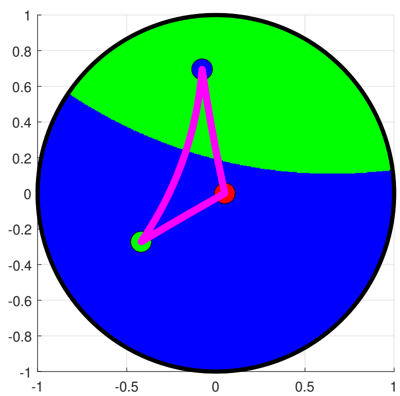

(b) Farthest-point Voronoi mapping generated by the pseudo hyperbolic distance. Vertices of the hyperbolic convex hull form a larger set than the range of V_A.

Fig. 4: Relationship between convex geometry and nonempty farthest-point Voronoi cells in the Euclidean and hyperbolic cases.

$$r_\alpha(z) = \sum_{n=0}^{\infty} \overline{\alpha}^n z^n \qquad (\alpha \in \mathbb{D}, |z| < 1)$$

it follows that the discrete Fourier coefficients of the elementary rational function r_α can be written as

$$\widehat{r}_{\alpha,N}(n) = \frac{\overline{\alpha}^n}{1-\overline{\alpha}^N} = \frac{\widehat{r}_\alpha(n)}{1-\overline{\alpha}^N} \qquad (0 \leq n < N). \tag{4.2}$$

Because of (4.2), we can use discrete Fourier coefficients to construct the ratios in (2.2).

In order to formulate the discrete Malmquist-Takenaka system, let us consider an N-periodic MT system $\phi^{\mathfrak{a}}_{n+Nk} = \phi^{\mathfrak{a}}_n B^k_{\mathfrak{a}}$ generated by the vector $\mathfrak{a} \in \mathbb{D}^N$. Taking the MTF coefficients of r_α and considering (2.10) leads to

$$\langle \phi^{\mathfrak{a}}_{n+Nk}, r_\alpha \rangle = \phi^{\mathfrak{a}}_n(\alpha) B^k_{\mathfrak{a}}(\alpha) \qquad (k \in \mathbb{N}, 0 \leq n < N). \tag{4.3}$$

Because $|B_{\mathfrak{a}}(\alpha)| < 1$, the Malmquist-Takenaka Fourier series with the coefficients (4.3) is absolutely and uniformly convergent on $\mathbb{T}$. Furthermore (since the MT system is complete in the Hardy space $H^2(\mathbb{D})$) the series produces r_α:

$$r_\alpha(z) = \sum_{n=0}^{N-1} \sum_{k=0}^{\infty} \overline{\phi}^{\mathfrak{a}}_n(\alpha)\phi^{\mathfrak{a}}_n(z) \overline{B}^k_{\mathfrak{a}}(\alpha) B^k_{\mathfrak{a}}(z) = \frac{1}{1-\overline{B}_{\mathfrak{a}}(\alpha)B_{\mathfrak{a}}(z)} \sum_{n=0}^{N-1} \overline{\phi}^{\mathfrak{a}}_n(\alpha)\phi^{\mathfrak{a}}_n(z). \tag{4.4}$$

Taking the limit $\alpha \to w \in \mathbb{T}$ in (4.4) produces the Christoffel-Darboux formula for Malmquist-Takenaka systems (seel also [5, 7, 28]):

$$\sum_{n=0}^{N-1} \overline{\phi}^{\mathfrak{a}}_n(w)\phi^{\mathfrak{a}}_n(z) = \frac{1-\overline{B}_{\mathfrak{a}}(w)B_{\mathfrak{a}}(z)}{1-\overline{w}z} \qquad (w, z \in \overline{\mathbb{D}}, w \neq z). \tag{4.5}$$

In order to acquire the discrete MT functions let us consider the set

$$\mathbb{T}^{\mathfrak{a}}_N := \{z \in \mathbb{T} : B_{\mathfrak{a}}(z) = 1\}, \tag{4.6}$$

where $\mathfrak{a} \in \mathbb{D}^N$. Since $B_{\mathfrak{a}} : \mathbb{T} \to \mathbb{T}$ is an N-fold mapping [25, 31], the number of elements in $\mathbb{T}^{\mathfrak{a}}_N$ is exactly N. We note that (4.6) can also be an appropriate choice of discretization points for a periodic MT system, whose period is less than N. For example, if we consider the 1-periodic (discrete Laguerre) system, choosing the discretization points (4.6) with $\mathfrak{a} = (a, a, a, a, \ldots) \in \mathbb{D}^N$ $(N \geq 1)$ is appropriate. Furthermore,

$$\sum_{n=0}^{N-1} \overline{\phi}^{\mathfrak{a}}_n(w)\phi^{\mathfrak{a}}_n(z) = \begin{cases} 0 & (z, w \in \mathbb{T}^{\mathfrak{a}}_N,\ z \neq w) \\ \sigma^2(z) & (z \in \mathbb{T}^{\mathfrak{a}}_N, z = w), \end{cases} \tag{4.7}$$

where

$$\sigma(z) := \sum_{n=0}^{N-1} \frac{1-|a_n|^2}{|1-\overline{a}_n z|^2}. \tag{4.8}$$

From the equations (4.7) and (4.8) it follows that the function system $\phi^{\mathfrak{a}}_n$ $(0 \leq n < N)$ is orthonormal with respect to the inner product

$$[f,g]_N^{\mathfrak{a}} := \sum_{z\in\mathbb{T}_N^{\mathfrak{a}}} f(z)\overline{g}(z)/\sigma(z), \tag{4.9}$$

or in other words $[\phi_n^{\mathfrak{a}},\phi_m^{\mathfrak{a}}]_N^{\mathfrak{a}} = \delta_{mn}$. Since $\phi_{n+kN}^{\mathfrak{a}} = \phi_n^{\mathfrak{a}}$ holds in any $z \in \mathbb{T}_N^{\mathfrak{a}}$ point, the discrete MTF coeffiecients are N-periodic. Using this and (4.4) we can arrive at a formula analogous to (4.2) for MTF coefficients:

$$[\phi_n^{\mathfrak{a}}, r_\alpha]_N^{\mathfrak{a}} = \frac{\overline{\phi}_n^{\mathfrak{a}}(\alpha)}{1-\overline{B}_{\mathfrak{a}}(\alpha)} = \frac{\langle \phi_n^{\mathfrak{a}}, r_\alpha\rangle}{1-\overline{B}_{\mathfrak{a}}(\alpha)} \quad (0\le n<N). \tag{4.10}$$

By (4.10) we can also use discrete MTF coefficients to construct the ratios needed for the proposed pole finding method (2.15).

5. Finding every pole of a rational function. In this section we are going to propose an iterative algorithm based on theorem 2.2, which allows for finding every inverse pole of a rational function R. As before, we are going to assume that every inverse pole is simple and denote the (finite) set of inverse poles by $A \subset \mathbb{D}$.

We begin by introducing a mechanism to eliminate inverse poles which have already been found. From section 3 it is clear that using p-periodic MTF coefficients in (2.15), where the MT system is generated by $\mathfrak{a} \in \mathbb{D}^p$ allows for the identification of a single $B_{\mathfrak{a}}$-dominant inverse pole. Modifying the parameter vector $\mathfrak{a}$ lets us find different inverse poles from A, however not every inverse pole can be acquired in this way (see figure 3). We will make use of the following observation:

$$B_{\mathfrak{a}}(\alpha) = 0 \qquad (\mathfrak{a} := (a_0,\ldots,a_{p-2},\alpha) \in \mathbb{D}^p, p\ge 1). \tag{5.1}$$

In effect (5.1) states that if the inverse pole $\alpha \in A$ is also a component of $\mathfrak{a}$, then α cannot be $B_{\mathfrak{a}}$-dominant. This provides an opportunity to "eliminate" already found inverse poles. Suppose we applied theorem 2.2 with a PMT system defined by $\mathfrak{a} \in \mathbb{D}^p$ to identify the inverse pole $\alpha \in \mathbb{D}$. Now applying (2.15) using the MTF coefficients determined by the vector $\mathfrak{b} := (\mathfrak{a},\alpha) \in \mathbb{D}^{p+1}$ guarantees by (5.1) that α cannot be found again. Repeating this process and considering larger p-periodic MT systems in each step allows us to find every inverse pole of R.

The question of when to stop the above described steps still needs to be considered. Many popular methods capable of identifying rational functions (for example the output error model [10]) assume the order of R to be known. If we can assume R has exactly $p \in \mathbb{N}$ poles, then it is possible to find every inverse pole of R by applying theorem 2.2 p times. In each step of this process, we can eliminate the inverse pole α found in the previous iteration by including it in the parameter vector that defines the current PMT system.

One advantage of our proposed pole finding scheme is that it is possible to apply theorem 2.2 without making any assumptions on the order of R. In this case however, one has to define a condition on when to stop looking for new inverse poles. We now propose one such possible stopping condition for the iterative application of theorem 2.2. Let $\phi_k(z) := \phi_k^{\mathfrak{a}_k}$, $\mathfrak{a}_k := (a_0,\ldots,a_{k-1})$, $(1\le k\le p)$ and consider the p-th Malmquist-Takenaka partial sum of R

$$S_pR(w) = S_p^{\mathfrak{a}}R(w) := \sum_{k=0}^{p-1} c_k\phi_k(w), \quad (R\in\mathcal{A},\ w\in\overline{\mathbb{D}}), \tag{5.2}$$

where c_k denote the k-th MTF coefficients.

Consider the H_2 norm

$$\|f\|_{H_2} = \sqrt{\langle f, f\rangle} \quad (f \in H_2(\mathbb{D}),$$

induced by the H_2 scalar product defined in (2.7). Clearly, if $\mathfrak{a}_p := (a_0, \ldots, a_{p-1})$ exactly matches the inverse poles of R, then $\|R - S_pR\|_{H^2} = 0$ is also true, therefore we can stop the iteration once the H^2 norm of $R - S_pR$ is zero. Since the inverse poles of R can are simple and are contained in $A = \{\alpha_0, \ldots, \alpha_{p-1}\} \subset \mathbb{D}^p$, the rational function R belongs to the subspace spanned by $\phi_0, \ldots, \phi_{p-1}$. Thus, $\|R-S_pR\|_{H^2} = 0$ indicates, that for the parameter vector generating the partial sum S_pR, we have $\mathfrak{a}_p = (\alpha_0, \ldots, \alpha_{p-1})$.

The steps for the k-th iteration of the proposed pole finding scheme can be summarized as follows.

1. Identify $\alpha_{k-1} \in A$, by applying theorem 2.2. Let the PMT system involved in the application of the theorem be generated by $\mathfrak{a}_k = (\alpha_0, \ldots, \alpha_{k-2}, a) \subset \mathbb{D}^k$, where $\alpha_0, \alpha_1, \ldots, \alpha_{k-2} \in A$.
2. Use the newly identified α_{k-1} inverse pole to construct the parameter vector $\mathfrak{b}_k := (\alpha_0, \alpha_k, \ldots, \alpha_{k-1}) \in \mathbb{D}^k$. Construct the PMT system $\phi_j(z) := \phi_j^{\mathfrak{b}_k}(z) \quad (j = 0, \ldots, k-1)$.
3. Consider the orthogonal projection of R onto the subspace spanned by $\phi_0^{\mathfrak{b}_k}, \phi_1^{\mathfrak{b}_k}, \ldots \phi_{k-1}^{\mathfrak{b}_k}$. This projection can be expressed by the formula in (5.2). The error of the projection is given by $\|R - S_kR\|_{H^2}$. If this error is zero, then we have successfully found every inverse pole of R (hence R is completely contained in the subspace), otherwise increase k and repeat the above steps.

In practice, we have to consider a discrete version of the problem. That is, suppose that instead of R, we only have access to the vector $\boldsymbol{r} \in \mathbb{C}^N \quad (N \in \mathbb{N})$, where the components of $\boldsymbol{r}$ are discrete samplings of R on $\mathbb{T}$. We may use an equidistant sampling of $\mathbb{T}$, or the discrete point set defined in (4.6). If we consider an equidistant sampling, we have to approximate the integrals $\langle \phi_{\nu_k}^{\mathfrak{a}}, R\rangle$ using a numerical quadrature such as the trapezoid rule when applying theorem 2.2. This approach is quick, however it introduces numerical errors especially for small N. Instead of this approach, we can also use the discrete scalar product and discrete orthogonal PMT systems as discussed in section 4. These allow us more precise computations from a numerical point of view. In this case however, we have to consider that each application of theorem 2.2 requires the calculation of the sampling points (4.6) as we modify the parameter vector defining the PMT system in each iteration of the proposed method. Thus, using discrete orthogonal PMT systems can increase computational cost. We note that since the error $\|R - S_pR\|_{H_2}$ depends heavily on R, many signal processing applications [8, 19] use normalized variations of it. In this work, we propose the use of percent root mean squared difference (PRD) (see e.g. [19]) to describe the error of the projection S_pR:

$$PRD(\mathfrak{a}) := \sqrt{\frac{\|R - S_p^{\mathfrak{a}}R\|_{H_2}^2}{\|R\|_{H_2}^2}} \cdot 100. \tag{5.3}$$

The use of the PRD score allows us to express the error of the approximation with percentages, thus we can construct a stopping condition for the proposed method that is usable for any R. In our future work we also plan to explore alternative stopping criteria suited for specific applications, however our experiments (see section 6) demonstrate the usefullness of the proposed approach (5.3). In a computer implementation of the proposed method, the norm $\|\cdot\|_{H_2}$ is replaced by the $\|\cdot\|_2$ vector norm, if R was sampled in an equidistant fashion or the norm induced by (4.9), if R was sampled on (4.6).

In algortithm 5.1 we summarize the steps of the proposed inverse pole identification and elimination approach. Algorithm 5.1 should not be considered a pseudo-code, rather a summary of the different steps needed to find the inverse poles of R. In this formulation we assumed the order of R to be unknown and relied on the above described exit condition to stop the iteration. For a more thorough consultation on the implementation, we refer to our MATLAB implementation of the proposed method [9].

Algorithm 5.1 Generalized Bernoulli's method to find every inverse pole

Obtain $\boldsymbol{r}$, a sampling of R on $\mathbb{T}$.
Let $PRD = 100$ and the exit condition $\varepsilon \in [0, 100]$.
Let $p = 1$.
Let $\mathfrak{a}$ and $\mathfrak{b}$ be empty vectors.
while $\varepsilon < PRD$ **do**

If $p = 1$, then let $\mathfrak{a} = (a) \in \mathbb{D}$. If $p > 1$, then let $\mathfrak{a} = (\mathfrak{b}_1, \ldots, \mathfrak{b}_{p-1}, a) \in \mathbb{D}^p$, where $\mathfrak{b}_k$ denotes the k-th component of the vector $\mathfrak{b}$. In either of these cases, a strategy to choose a is given in section 6.

Obtain α_{p-1} by applying theorem 2.2 with $\mathfrak{a}$. The practical application of theorem 2.2 is discussed in section 6.

If $p = 1$, then let $\mathfrak{b} = (\alpha_{p-1}) \in \mathbb{D}$. If $p > 1$, then let $\mathfrak{b} = (\mathfrak{b}_1, \ldots, \mathfrak{b}_{p-1}, \alpha_{p-1}) \in \mathbb{D}^p$. The vector $\mathfrak{b}$ contains the already found inverse poles.

Calculate a discrete version of the projection $S_p^{\mathfrak{b}} R$.

Let $PRD = PRD(\mathfrak{b})$, where the function $PRD(\mathfrak{b})$ is defined in (5.3).

Let $p = p + 1$.

end while

6. Numerical considerations. In this section we consider some practical problems that arise when we implement the proposed pole finding scheme. Namely, we investigate the behavior of the ratios in (2.15), when we can only calculate the MTF coefficients up to some finite index. In addition, we propose a strategy to choose the parameter vector $\mathfrak{a} \in \mathbb{D}^p$ that defines the Malmquist-Takenaka system in the p-th step of algorithm 5.1.

For a function $f \in H^2(\mathbb{D})$, the modulus of the periodic Malmquist-Takenaka Fourier coefficients $c_n^{\mathfrak{a}} := \langle \phi_n^{\mathfrak{a}}, f \rangle$ tends quickly to zero if $n \to \infty$. This behavior means that as k increases, calculating the ratios

$$s_k(\mathfrak{a}) := c_{\nu_k}^{\mathfrak{a}} / c_{\nu_k - 1}^{\mathfrak{a}} \tag{6.1}$$

incurs large numerical errors. On the other hand, considering ratios where the indices ν_k are too small, the values (6.1) may not approximate the limit well. This problem is illustrated in Figure 5.

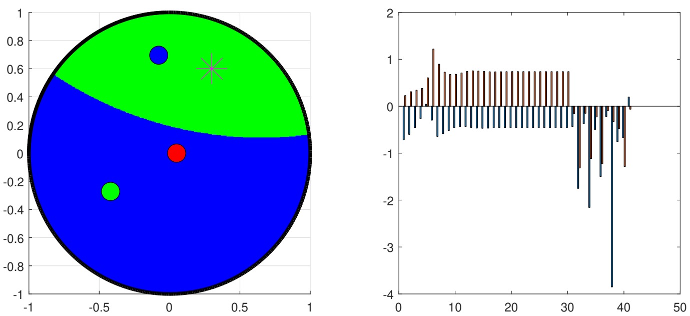

Fig. 5: LEFT: Inverse poles of R (small circles) and the parameter of the PMT system (star) for $p = 1$. RIGHT: Real and imaginary parts of the ratios (6.1). If the index k is too small, the ratios oscillate, and if it is too large numerical errors begin to appear.

In order to select the ratios which approximate the limit $s(\mathfrak{a}) := \lim_{k\to\infty} s_k(\mathfrak{a})$ closely enough, we have to find an interval $J = [k, k+\ell]$ of indices, where $s_k(\mathfrak{a})$ exhibit "near constant" behavior. To do this, we propose to measure the oscillation in the window J by

$$\omega(J, \mathfrak{a}) := \max_{i,j\in J} |s_i(\mathfrak{a}) - s_j(\mathfrak{a})|. \tag{6.2}$$

For a fixed $\mathfrak{a}$ we can approximate the limit of (6.1) using

$$\omega^*(\mathfrak{a}) = \min_J \omega(J, \mathfrak{a}) = \omega([m^*, m^* + \ell], \mathfrak{a}), \quad s(\mathfrak{a}) \approx s_{m^*}(\mathfrak{a}). \tag{6.3}$$

As shown in section 2, the inverse pole can be recovered by

$$\alpha_0 = Q^{\mathfrak{a}}(s(\mathfrak{a})),$$

where the mapping $Q^{\mathfrak{a}}$ is defined in (2.17). Consequently, the error formula (2.20) given as

$$|Q^{\mathfrak{a}}(s(\mathfrak{a})) - Q^{\mathfrak{a}}(s_{m^*}(\mathfrak{a}))| \le M(\mathfrak{a}) \cdot |s(\mathfrak{a}) - s_{m^*}(\mathfrak{a})|$$

can be used to estimate the error of the reconstruction, where $M(\mathfrak{a})$ is defined in (2.21). Unfortunately, in practice we cannot calculate the exact value of $s(\mathfrak{a})$. In this work, we approximate the error $|s_k(\mathfrak{a}) - s(\mathfrak{a})|$ with $|s_k(\mathfrak{a}) - s_{k+l}(\mathfrak{a})|$ $(l, k \in \mathbb{N})$. We now proceed to show that this error decreases quickly and is therefore appropriate for most practical cases. By theorem 2.2, there exists $0 \le q < 1$ and $M \in \mathbb{R}$ for which

$$|s_k(\mathfrak{a}) - s(\mathfrak{a})| \le M \cdot q^k \quad (k \in \mathbb{N}). \tag{6.4}$$

From this, we get

$$\begin{aligned} |s_k(\mathfrak{a}) - s_{k+l}(\mathfrak{a})| &\le M(q+1) \cdot \left(q^k + q^{k+1} + \ldots\right) \\ &= M \cdot q^k \cdot \frac{1+q}{1-q} \quad (l > 0). \end{aligned} \tag{6.5}$$

By (6.5), the proposed practical error estimate $|s_k(\mathfrak{a}) - s_{k+l}(\mathfrak{a})|$ has the same order of decay as $|s_k(\mathfrak{a}) - s(\mathfrak{a})|$ and can be used in applications. If q is close to 1, then the proposed estimate is not as reliable, however we did not see a large difference between the proposed estimate $|s_k(\mathfrak{a}) - s_{k+l}(\mathfrak{a})|$ and the actual error (6.4) in our experiments. Finally, we remark, that the MTF coefficients contain information about *every pole* of R. Methods for the $p = 1$ case have already been developed, where multiple poles are identified using the PMT expansion of R with $p = 1$ [13]. Based on our numerical experiments, we conjuncture that if we approximate $s(\mathfrak{a})$ with $s_n(\mathfrak{a})$, where $s_n(\mathfrak{a})$ falls into a "relatively constant" part of the sequence $s_k(\mathfrak{a})$, then $Q^{\mathfrak{a}}(s_n(\mathfrak{a}))$ will approximate *one of the inverse poles* of R (not necessarily α_0). We plan to study this phenomenon and formalize our findings in a future work.

We found in our experiments that estimating the value of the error formula (2.20) with

$$E(m^*, \mathfrak{a}) := M(\mathfrak{a}) \cdot \omega^*(\mathfrak{a}) \tag{6.6}$$

suffices whenever the order of R is not too large.

Next, we propose an approach to automatically choose the parameter $\mathfrak{a} \in \mathbb{D}^p$ in the p-th step of algorithm 5.1. By the error formulas (2.20) and (6.6) it is clear that the error of the inverse pole reconstruction depends heavily on the parameter vector $\mathfrak{a}$. A poor choice of $\mathfrak{a}$ can mean that the sequence (6.1) converges slowly. This phenomenon is illustrated in figure 6. In this sense we can find a good parameter vector $\mathfrak{a}$ by minimizing the function

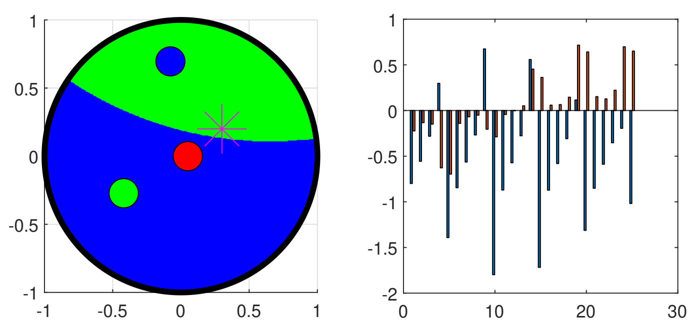

Fig. 6: LEFT: Inverse poles of R (small circles) and the parameter of the PMT system (star) for $p = 1$. RIGHT: Real and imaginary parts of the ratios (6.1). If the parameters of the PMT system lie close to the border of the Voronoi cells discussed in section 3, then convergence of the ratios (6.1) is slow.

$$E_{m^*}(\mathfrak{a}) := E(m^*, \mathfrak{a}), \tag{6.7}$$

where, for any given $\mathfrak{a}$, the index m^* is determined by (6.3). Minimizing (6.7) leads to a nonlinear optimization problem. We note that in the p-th step of the algorithm, the first $p - 1$ components of $\mathfrak{a}$ are fixed (they are the inverse poles reconstructed in previous steps), therefore we only have to find a single $a_p \in \mathbb{D}$ parameter which minimizes (6.7). In this work we considered two algorithms to solve the above mentioned optimization problem. In the first case, we considered 10 random $a \in \mathbb{D}$ at each step of the algorithm and selected the one for which (6.7) was minimal. In the second case, we used the hyperbolic variant of the Nelder-Mead simplex method [23]. The Nelder-Mead method [26] can be used to solve nonlinear optimization problems. It applies successive geometric transformations to a simplex, whose vertices represent the current state of the minimization. The applied transformations depend on the objective function's values at the vertices. The hyperbolic Nelder-Mead algorithm introduced in [23] replaces these geometric transformations with their hyperbolic variants. When minimizing the objective (6.7) this is useful, as it naturally ensures all components of the vector $\mathfrak{a}$ remain strictly inside $\mathbb{D}$. We note that the proof of convergence can only be given in simple cases, even in the original variant of the Nelder-Mead method (see e.g. [23]). Despite this, it remains a popular minimization method based on empirical evidence and the results of our experiments also confirm its usefulness for the problem stated above. In particular, our below numerical results demonstrate the effectiveness of the proposed method when used with the above mentioned optimization schemes.

We created a MatLab implementation of the proposed methods which can be accessed at [9]. To calculate periodic MT systems and the corresponding coefficients, we relied on the library introduced in [21]. Below, we provide an example to demonstrate the effectiveness of the proposed algorithm. We consider the rational function R given by the inverse poles $A := \{0.3 + 0.4i,\ -0.5 - 0.4i,\ 0.7 - 0.3i\}$ and zeros $z_0 = 0.8 + 0.4i, z_1 = 0.8 + 0.4i$. We choose parameter $\mathfrak{a}$ in each step of the algorithm by minimizing (6.7) by the above described optimization methods. The results for this example can be found in table 1. The rows of the table represent the iterations of algorithm 5.1.

	Hyperbolic Nelder Mead		Monte Carlo optimization	
Step	$\boldsymbol{\lvert\alpha_0 - Q^{\mathfrak{a}}(s_{m^*}(\mathfrak{a}))\rvert}$	$\boldsymbol{E_{m^*}(\mathfrak{a})}$	$\boldsymbol{\lvert\alpha_0 - Q^{\mathfrak{a}}(s_{m^*}(\mathfrak{a}))\rvert}$	$\boldsymbol{E_{m^*}(\mathfrak{a})}$
1	$5.03 \cdot 10^{-12}$	$4.26 \cdot 10^{-11}$	$1.86 \cdot 10^{-9}$	$1.83 \cdot 10^{-8}$
2	$5.02 \cdot 10^{-15}$	$3.73 \cdot 10^{-14}$	$5.39 \cdot 10^{-11}$	$2.71 \cdot 10^{-10}$
3	$1.48 \cdot 10^{-15}$	$1.35 \cdot 10^{-14}$	$1.04 \cdot 10^{-15}$	$1.28 \cdot 10^{-14}$

Table 1: Results for the above described example problem. The columns $|\alpha_0 - Q^{\mathfrak{a}}(s_{m^*}(\mathfrak{a}))|$ and $E_{m^*}(\mathfrak{a})$ refer to the actual error of the reconstruction and the error estimate with the optimized parameters (6.6).

In table 2, we present the results of a larger simulation. In this case, we constructed rational functions of the form $R(z) := \sum_{k=1}^{M} c_k \cdot r_{\alpha_k}(z) \quad (c_k \in \mathbb{C}, \alpha_k \in \mathbb{D}, z \in \overline{\mathbb{D}})$, where the coefficients c_k and the inverse poles α_k were chosen randomly. We conducted 100 such experiments for each $M = 1, \ldots, 5$, with table 2 showing the mean distance of the estimates from the actual inverse poles of R. The proposed method was applied with hyperbolic Nelder-Mead optimization. To simplify the evaluation of the results, the number of poles of R was assumed to be known in these experiments. In table 2, the error values for each M are given by

$$\mathrm{Err}(M) := \frac{1}{100} \sum_{k=1}^{100} \left(\frac{1}{M} \sum_{j=0}^{M-1} |\alpha_{k,j} - Q^{\mathfrak{a}}_{k,j}(s_{m^*}(\mathfrak{a}))| \right), \tag{6.8}$$

where $\alpha_{k,j}$ denotes the j-th inverse pole of the k-th rational function which is defined by M poles and $Q^{\mathfrak{a}}_{k,j}(s_{m^*}(\mathfrak{a}))$ denotes the estimate of $\alpha_{k,j}$ produced by our proposed method. The results in table 2 show, that our proposed method can be used reliably to find the inverse poles of R. For elementary rational functions (when $M = 1$), the reconstruction is almost perfect even for a large number of experiments. When increasing the number of inverse poles that define R, we can see a decrease in precision, however the average error defined in (6.8) remains in the order of 10^{-5} even if $M = 5$.

Finally, we conducted an experiment to measure the effectiveness of the stopping criteria for our algorithm proposed in section 5. In particular we generated 100 rational functions, each with 5 poles and applied the proposed method to find every inverse pole. This time however, we did not assume the number of poles to be known in advance, instead we stopped our iteration once the value of the PRD error (5.3) became less than $\varepsilon = 10$. We found that the average number of identified inverse poles throughout the 100 experiments in this case was 4.3. A perfect score could not be expected, because some inverse poles contribute very little to the energy ($\|R\|_{H_2}$) of R, however the results show that we can rely on this scheme to accurately identify most significant inverse poles. We note that lowering the threshold ε increases the number of identified inverse poles, however it also increases computational cost (as the algoirthm will keep looking for new inverse poles even after the most dominant ones have been found).

M	1	2	3	4	5
Err(M) see (6.8)	$3.0 \cdot 10^{-16}$	$1.5 \cdot 10^{-6}$	$4.2 \cdot 10^{-7}$	$1.9 \cdot 10^{-5}$	$2.9 \cdot 10^{-5}$

Table 2: Results of a larger experiment with different numbers of poles.

In our experiments we found that the proposed algorithm can be used to reliably identify the inverse poles of rational functions. Even though both described optimization methods provided good estimates on the inverse poles, applying the hyperbolic variant of the Nelder-Mead optimization showed slightly better precision. In the experiment detailed in table 1, the average distance between the estimated and true inverse poles was $1.68 \cdot 10^{-12}$ with the Nelder-Mead method and $6.39 \cdot 10^{-10}$ if we used a Monte Carlo approach. Every experiment was conducted using the algorithm in our implementation [9]. The above results justify using nonlinear optimization algorithms adapted to hyperbolic geometry to minimize (6.7). In our future work, we plan to experiment using further hyperbolic optimization methods such as [20].

7. Conclusion. In this work we introduced a generalization of Bernoulli's classical method of finding the poles of a rational function. The generalization uses periodic Malmquist-Takenaka Fourier coefficients to construct the sequence of ratios used by Bernoulli's original algorithm. We generalized the concept of dominant poles using Blaschke-products and gave a description of the poles which can be found with the proposed method. Furthermore, we showed that discrete orthogonal Malmquist-Takenaka systems can also be used with the proposed method. Using our results, we proposed an iterative algorithm which applies the generalized Bernoulli's method to find every inverse pole of the rational function. Finally, we proposed a method to automatically select the parameters of our algorithm by minimizing an intuitive cost function with different optimization techniques.

The proposed method is an interesting generalization of a classical numerical algorithm, which in our opinion is worthy of attention by itself. In addition however, the proposed method exhibits great practical potential in the field of system identification. Specifically, in our future work we plan to investigate ways in which to apply the proposed algorithm to identify the poles of the transfer functions of SISO-LTI (single input single output, linear time invariant) systems [2]. One promising property of the proposed algorithm is that the order of the transfer function to be identified need not be known in advance.

Another area of future investigation will be the description of identifiable inverse poles through convex geometry. As mentioned in section 3, when the generalized algorithm is used with Laguerre (1-periodic Malmquist-Takenaka) Fourier coefficients, the set of identifiable inverse poles can be given by calculating their so-called paracyclic convex hull. This result and further generalizations for the case $p > 1$ will be considered in our future research.

Acknowledgments. Project no. C1748701, K146721 have been implemented with the support provided by the Ministry of Culture and Innovation of Hungary from the National Research, Development and Innovation Fund, financed under the NVKDP-2021 and the K_23 "OTKA" funding schemes, respectively. The research was supported by the European Union within the framework of the National Laboratory for Autonomous Systems. (RRF-2.3.1-21-2022-00002).

REFERENCES

[1] A. Aitken, *On Bernoulli's numerical solution of algebraic equations.-Proc. Roy. Soc., Edinburgh, ser. a, 46*, (1925).
[2] K. J. Åström and R. M. Murray, *Feedback systems: an introduction for scientists and engineers*, Princeton university press, 2021.
[3] W. Blaschke, *Eine Erweiterung des Satzes von Vitali über Folgen analytischer Funktionen*, In: Ber. Verhandl. Kön. Sächs. Ges. Wiss. Leipzig, 67 (1915), pp. 194–200.
[4] K. Q. Brown, *Voronoi diagrams from convex hulls*, Information processing letters, 9 (1979), pp. 223–228.
[5] A. Bultheel, P. González-Vera, E. Hendriksen, and O. Njastad, *Orthogonal rational functions*, Cambridge University Press, 1999.
[6] H. S. M. Coxeter, *Non-Euclidean geometry*, Cambridge University Press, 1998.
[7] M. Djrbashian, *Orthogonal systems of rational functions on the circle*, Izv. Akad. Nauk Armyan. SSR, 1 (1966), pp. 3–24.
[8] T. Dózsa, J. Radó, J. Volk, A. Kisari, A. Soumelidis, and P. Kovács, *Road abnormality detection using piezoresistive force sensors and adaptive signal models*, IEEE Transactions on Instrumentation and Measurement, 71 (2022), pp. 1–11.
[9] T. Dózsa, F. Schipp, and A. Soumelidis, *On Bernoulli's method*, 2022, https://codeocean.com/capsule/1628672/tree.
[10] H. Duan, J. Jia, and R. Ding, *Two-stage recursive least squares parameter estimation algorithm for output error models*, Mathematical and Computer Modelling, 55 (2012), pp. 1151–1159.
[11] C. Gasquet and P. Witomski, *Fourier analysis and applications: filtering, numerical computation, wavelets*, vol. 30, Springer Science & Business Media, 2013.
[12] A. Gopal and L. N. Trefethen, *Solving Laplace problems with corner singularities via rational functions*, SIAM Journal on Numerical Analysis, 57 (2019), pp. 2074–2094.
[13] I. Gőzse and A. Soumelidis, *Realizing system poles identification on the unit disc based on the Fourier trasform of Laguerre-coefficients*, in 2015 23rd Med. Conf. on Control and Automation (MED), 2015, pp. 821–826.
[14] P. Henrici, *Elements of numerical analysis*, John Wiley & Sons, 1964.
[15] P. Henrici, *Applied and computational complex analysis, Volume 1*, John Wiley & Sons, 1974.
[16] P. S. Heuberger, P. M. Van den Hof, and B. Wahlberg, *Modelling and identification with rational orthogonal basis functions*, Springer Science & Business Media, 2005.
[17] A. S. Householder, *The numerical treatment of a single nonlinear equation*, McGraw-Hill, 1970.
[18] J. König, *Über eine Eigenschaft der Potenzreihen*, Mathematische Annalen, 23 (1884), pp. 447–

449.
[19] P. Kovács, S. Fridli, and F. Schipp, *Generalized rational variable projection with application in ecg compression*, IEEE Transactions on Signal Processing, 68 (2020), pp. 478–492.
[20] P. Kovács, S. Kiranyaz, and M. Gabbouj, *Hyperbolic particle swarm optimization with application in rational identification*, in 21st European Signal Processing Conference (EUSIPCO 2013), IEEE, 2013, pp. 1–5.
[21] P. Kovács and L. Lócsi, *Rait: the rational approximation and interpolation toolbox for Matlab, with experiments on ECG signals*, International Journal of Advances in Telecommunications, Electrotechnics, Signals and Systems, 1 (2012), pp. 67–75.
[22] B. Le Bailly and J.-P. Thiran, *Optimal rational functions for the generalized Zolotarev problem in the complex plane*, SIAM Journal on Numerical Analysis, 38 (2000), pp. 1409–1424.
[23] L. Lócsi, *A hyperbolic variant of the Nelder-Mead simplex method in low dimensions*, Acta Univ. Sapientiae, Math, 5 (2013).
[24] F. Malmquist, *Sur la détermination d'une classe de fonctions analytiques par leurs valeurs dans un ensemble donné de points*, In Comptes Rendus du Sixième Congrès des mathématiciens scandinaves, (1925), pp. 253–259.
[25] J. Mashreghi, E. Fricain, et al., *Blaschke products and their applications*, Springer, 2013.
[26] J. A. Nelder and R. Mead, *A simplex method for function minimization*, The computer journal, 7 (1965), pp. 308–313.
[27] R. Pachón, P. Gonnet, and J. Van Deun, *Fast and stable rational interpolation in roots of unity and Chebyshev points*, SIAM Journal on Numerical Analysis, 50 (2012), pp. 1713–1734.
[28] M. Pap and F. Schipp, *Equilibrium conditions for the Malmquist-Takenaka systems*, Acta Scientiarum Mathematicarum, 81 (2015), pp. 469–482.
[29] H. Rutishauser, *Der Quotienten-Differenzen-Algorithmus*, Zeitschrift für angewandte Mathematik und Physik ZAMP, 5 (1954), pp. 233–251.
[30] H. Rutishauser, *Der Quotienten-Differenzen-Algorithmus*, Springer, 1957.
[31] F. Schipp, *Hyperbolic wavelets*, in Topics in Mathematical Analysis and Applications, Springer, 2014, pp. 633–657.
[32] F. Schipp and A. Soumelidis, *On the Fourier coefficients with respect to the discrete Laguerre system*, Annales Univ. Sci. Budapest., Sect. Comp, 34 (2011), pp. 223–233.
[33] F. Schipp and A. Soumelidis, *Eigenvalues of matrices and discrete Laguerre-Fourier coefficients*, Mathematica Pannonica, 147 (2012), p. 155.
[34] Z. Szabó and J. Bokor, *Non-Euclidean Geometries in Modeling and Control*, Széchenyi University Press, Győr, Hungary, 2015.
[35] S. Takenaka, *On the orthogonal functions and a new formula of interpolation*, in Japanese journal of mathematics: transactions and abstracts, vol. 2, The Mathematical Society of Japan, 1925, pp. 129–145.
[36] S. Takenaka, *On the orthogonal functions and a new formula of interpolations*, Japanese Journal of Mathematics, 2 (1925), pp. 129–145.
[37] L. N. Trefethen, *Numerical conformal mapping with rational functions*, Computational Methods and Function Theory, 20 (2020), pp. 369–387.
[38] L. N. Trefethen, Y. Nakatsukasa, and J. Weideman, *Exponential node clustering at singularities for rational approximation, quadrature, and pdes*, Numerische Mathematik, 147 (2021), pp. 227–254.
[39] D. Xiong, L. Chai, and J. Zhang, *Sparse system identification in pairs of pulse and Takenaka-Malmquist bases*, SIAM Journal on Control and Optimization, 58 (2020), pp. 965–985.